CHEMISTRY
A EUROPEAN JOURNAL

DOI: 10.1002/chem.200900764

The Protonation of HSO_3F: Preparation and Characterization of Fluorodihydroxyoxosulfonium Hexafluoroantimonate $[H_2SO_3F]^+[SbF_6]^-$

Raphael Seelbinder,[b] Nadine R. Goetz,[a] Johannes Weber,[a] Rolf Minkwitz,[b] and Andreas J. Kornath*[a]

Dedicated to Professor Ingo-Peter Lorenz on the occasion of his 65th birthday

Abstract: Sulfurtrioxide reacts with the superacidic solutions XF/SbF_5 (X = H, D) to form the corresponding salts $[X_2SO_3F]^+[SbF_6]^-$, which are the protonated forms of fluorosulfuric acid. The salts have been characterized by vibrational spectroscopy and a single-crystal structure analysis. $[H_2SO_3F]^+[SbF_6]^-$ crystallizes in the monoclinic space group $P2_1/n$ (no. 14) with four formula units in the unit cell. The crystal structure possesses a distorted tetrahedral O_3SF skeleton of the cations, which are linked with two strong hydrogen bridges to $[SbF_6]^-$ anions and forms a one-dimensional chain. The crystal structure and the vibrational spectra are compared to the quantum-chemical-calculated free $[H_2SO_3F]^+$ cation. Additionally, an $[H_2SO_3F(HF)_2]^+$ unit was calculated at the RHF/6-311++G(d,p) level to simulate H···F hydrogen bridges found in the solid state.

Keywords: fluorosulfuric acid · quantum chemistry · structure elucidation · superacidic systems · vibrational spectroscopy

Introduction

The chemistry in liquid superacid media has been investigated extensively since 1960.[1,2] The characterization of the superacids themselves and the characterization of reactive species in superacidic solutions by vibrational spectra and NMR spectroscopic techniques is well established and has resulted in a large number of interesting onium ions.[1–4] The isolation of the reactive species of the superacids, which are in many cases protonated compounds, offers the possibility of X-ray investigations that lead to the structural characterization of the resulting salts. In the past, salts of protonated weak bases have been isolated, among them salts of protonated acids such as acetic acid, formic acid, or phosphoric acid.[5–7]

The preparation and isolation of $[H_3SO_4]^+[SbF_6]^-$ has demonstrated that even such weak bases as sulfuric acid can be protonated by HF/SbF_5 superacidic solutions.[8] The acid strength of pure sulfuric acid constitutes, by definition, the border to the superacids.[1,2,9–12] On the Hammett acidity scale sulfuric acid reaches an H^0 value of -12.1.[1,2] Acids with a lower H^0 value than that of sulfuric acid are superacids. The successful synthesis of $[H_3SO_4]^+[SbF_6]^-$ leads to the general question whether even stronger acids such as fluorosulfuric acid ($H^0 = -15.1$) can be protonated and the resulting salts isolated.

It is generally accepted that fluorosulfuric acid undergoes an autoprotolysis during the formation of $[SO_3F]^-$ anions and $[H_2SO_3F]^+$ cations with a concentration of 3.5×10^{-4} mol L^{-1} of each ion.[11] The spectroscopic and structural properties of the pure acid and the $[SO_3F]^-$ anion are well known,[13–18] but the existence of $[H_2SO_3F]^+$ is only assumed on the basis of cryoscopic and conductivity measurements.[11] ^1H and ^{19}F NMR spectroscopy experiments in superacidic solutions of the magic acid HSO_3F/SbF_5 have been performed. Although the concentration of the cation is much higher in magic acid than in pure fluorosulfuric acid, $[H_2SO_3F]^+$ was deemed indistinguishable from HSO_3F due to the rapid proton transfer and to the fact that the salt was not successfully isolated.[19–22] This lack of evidence for the

[a] N. R. Goetz, Dr. J. Weber, Prof. Dr. A. J. Kornath
Ludwig-Maximilians-University of Munich
Department of Chemistry and Biochemistry, Inorganic Chemistry
Butenandtstrasse 5–13, 81377 Munich (Germany)
Fax: (+49) 89-218 077 487
E-mail: andreas.kornath@cup.uni-muenchen.de

[b] Dr. R. Seelbinder, Prof. Dr. R. Minkwitz
Technical University of Dortmund
Faculty of Chemistry, Inorganic Chemistry
Otto-Hahn-Strasse 6, 44221 Dortmund (Germany)

$[H_2SO_3F]^+$ cation prompted us to investigate the reaction of fluorosulfuric acid in the superacidic system HF/SbF_5.

Results and Discussion

Synthesis and properties of $[H_2SO_3F]^+[SbF_6]^-$: The salt was prepared in a quantitative yield in a two-step synthesis according to Equations (1) and (2):

$$2\,HF + SbF_5 \xrightarrow{RT} [H_2F]^+[SbF_6]^- \quad (1)$$

$$[H_2F]^+[SbF_6]^- + SO_3 + HF \xrightarrow{-35\,^\circ C} [H_2F]^+[SbF_6]^- + HSO_3F \xrightleftharpoons{-78\,^\circ C} [H_2SO_3F]^+[SbF_6]^- + HF \quad (2)$$

In the first step, the superacid HF/SbF_5 was formed to ensure the highest possible concentration of $[H_2F]^+[SbF_6]^-$ in a homogeneous HF solution. In the second step, SO_3 was condensed to the frozen superacid instead of HSO_3F, which is less volatile and difficult to condense quantitatively on a vacuum line. During the warm-up process of the reaction mixture, the superacid melted, and at −35 °C a part of the HF excess ($SbF_5/HF = 1:150$) reacted with the solid SO_3 during formation of fluorosulfuric acid, which was then protonated by the simplified equilibrium shown in Equation (2). It is unknown to what extent fluorosulfuric acid is protonated in this solution, but after removal of the excess of HF at −78 °C, only colorless crystals of $[H_2SO_3F]^+[SbF_6]^-$ remained. Probably, the isolation of pure $[H_2SO_3F]^+[SbF_6]^-$ succeeded, because the simplified equilibrium [Eq. (2)] shifted to the product side by precipitation of $[H_2SO_3F]^+[SbF_6]^-$ during removal of HF. The colorless, crystalline, and extremely moisture-sensitive salt was stable below −70 °C. Hydrolysis led, even at low temperatures, to the formation of $[H_3O]^+[SbF_6]^-$ and HSO_3F.

The successful synthesis of $[H_2SO_3F]^+[SbF_6]^-$ is in agreement with earlier studies and indicates that the conjugated Brønsted–Lewis superacid HF/SbF_5 is more acidic than HSO_3F/SbF_5. Both pure fluorosulfuric acid and hydrogen fluoride have an H^0 value of −15.1. The acidities of both acids increased upon the addition of SbF_5 but to different extents. A 1 M solution of SbF_5 in HF is about 10^4 times stronger than a solution of HSO_3F that contains the same amount of SbF_5.[1] For more concentrated solutions, only kinetic data are available, from which it has been estimated that HF/SbF_5 is more acidic than HSO_3F/SbF_5. Nevertheless, these results have sometimes been questioned, since measurements in these acidity ranges bear difficulties and may be not comparative. So far, the successful synthesis of $[H_2SO_3F]^+[SbF_6]^-$ supports earlier studies, since, finally, the more acidic superacid HF/SbF_5 protonates the weaker HSO_3F/SbF_5 system.

Crystal structure of $[H_2SO_3F]^+[SbF_6]^-$: The crystal data are summarized in Table 1.[23] Fluorodihydroxyoxosulfonium hexafluoroantimonate crystallizes in the monoclinic space group $P2_1/n$ (no. 14) with four formula units per cell. For the data collection, reduction, structure solution, and refinement, SCALEPACK, programs in the SHELXTL package, PARST, and PLATON were used.[24–27] The antimony layers were found by the Patterson method. All atoms including protons were found in the difference Fourier synthesis. All non-hydrogen atoms were refined with anisotropic thermal parameters.

Table 1. Crystal data and structure refinement for $[H_2SO_3F]^+[SbF_6]^-$.

empirical formula	$H_2F_7O_3SSb$
M_r	336.83
T [K]	173(2)
wavelength [pm]	71.073
crystal system	monoclinic
space group	$P2_1/n$
a [pm]	665.8(1)
b [pm]	1343.8(1)
c [pm]	817.00(1)
β [°]	91.939(1)
V [Å^3]	730.6(2)
Z	4
ρ_{calcd} [g cm^{-3}]	3.062
absorption coefficient [mm^{-1}]	4.167
$F(000)$	624
θ range [°]	2.92–26.50
index ranges	$-9 \le h \le 7$, $-16 \le k \le 18$, $-10 \le l \le 11$
reflections collected	4011
independent reflections	1494 (R(int) = 0.0269)
refinement method	full-matrix least-squares on F^2
data/restraints/parameters	1470/0/112
goodness-of-fit on F^2	1160
final R indices ($I > 2\sigma(I)$)[a]	$R1 = 0.0179$, $wR2 = 0.0408$
R indices (all data)[a]	$R1 = 0.0240$, $wR2 = 0.1275$
extinction coefficient	0.0308(9)
largest diff. peak and hole [e Å^{-3}]	0.457 and −0.713

[a] $R = \Sigma||F_o| - |F_c||/\Sigma|F_o|$.

Bond lengths and selected angles of $[H_2SO_3F]^+[SbF_6]^-$ are summarized in Table 2. The structure of the $[H_2SO_3F]^+$ cation and its hydrogen bonds to the nearest fluorine atoms of the anions, together with the calculated $[H_2SO_3F(HF)_2]^+$ structure, which will be discussed later, are shown in Figure 1. Figure 2 shows a section of the crystal structure.

Table 2. Selected bond lengths [pm] and angles [°] for $[H_2SO_3F]^+[SbF_6]^-$.

S(1)–O(3)	139.5(3)	O(3)-S(1)-O(1)	119.1(2)
S(1)–O(1)	147.5(3)	O(3)-S(1)-O(2)	117.6(2)
S(1)–O(2)	148.5(3)	O(1)-S(1)-O(2)	103.3(1)
S(1)–F(7)	150.9(2)	O(3)-S(1)-F(7)	110.0(2)
O(1)–H(1)	75.6(3)	O(1)-S(1)-F(7)	101.8(2)
O(2)–H(2)	93.1(2)	O(2)-S(1)-F(7)	102.7(1)
		S(1)-O(1)-H(1)	109.6(2)
		S(1)-O(2)-H(2)	120.6(2)
Sb(1)–F(2)	191.6(2)	F(3)-Sb(1)-F(1)	176.6(1)
Sb(1)–F(1)	192.6(2)	F(2)-Sb(1)-F(1)	87.4(1)

In the $[H_2SO_3F]^+[SbF_6]^-$ salt, one S=O bond with 139.5(3) pm and two S–O bonds with lengths of 147.5(3) and 148.5(3) pm are observed. These lengths are in the

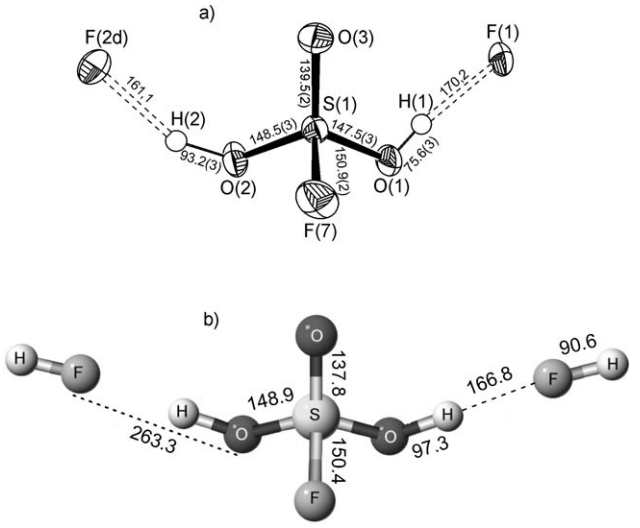

Figure 1. a) A fragment of the crystal structure of $[H_2SO_3F]^+[SbF_6]^-$ showing the $[H_2SO_3F]^+$ cation with interionic contacts [pm] (50% probability ellipsoids for the non-hydrogen atoms); symmetry operations: $d = x+1/2, -y+1/2, z+1/2$. b) The ab initio calculated structure (RHF/6-311++G(d,p)) of the $[H_2SO_3F(HF)_2]^+$ unit.

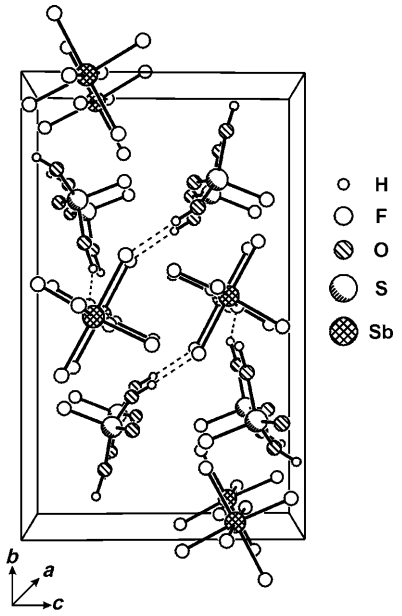

Figure 2. Projection of the $[H_2SO_3F]^+[SbF_6]^-$ salt with interionic contacts.

region typical for SO single and double bonds, respectively, and comparable to the corresponding SO bonds in the $[D_3SO_4]^+$ cation.[8] The S–F bond length of 150.9(2) pm is in the typical region of S–F bonds. As expected for a cation, the comparable S–O, S=O, and S–F bond lengths are slightly shorter than in the HSO_3F molecule.[13] The S–F and S–O bonds of the $[H_2SO_3F]^+$ cation have similar bond lengths, thus crystallographic disorder could be assumed. This assumption can be rejected by taking into account the environment of the oxygen and fluorine atoms of the cation. The found O–H lengths of 75.6(3) and 93.1(2) pm are very short. However, they are not meaningful for the structure of the salt and therefore do not significantly support the localization of the oxygen atoms. However, the oxygen atoms have O···F contacts to the anions of 244.8 and 248.7 pm, which are in the range of short hydrogen bonds (O···H···F) like those found, for example, in $[D_3SO_4]^+[SbF_6]^-$ and $[H_2SO_2F]^+[SbF_6]^-$.[8,28] On the other hand, the shortest F···F distance between anion and cation is 295.0 pm.

Because of the steric demand of the S=O double bond on the sulfur atom, the O-S-F angles are compressed to 101.8(2) and 102.7(1)°, and the O-S-O angle to 103.3(1)°, from the ideal tetrahedral geometry. The cations are linked by two strong O···H···F hydrogen bridges with $[SbF_6]^-$ anions to one-dimensional wavy strands stacked parallel in the *a* and *b* axis. The Sb–F bonds taking part in the hydrogen bridges (191.6(2) and 192.6(2) pm) are significantly longer than the Sb–F bonds (184.8(2) and 186.2(2) pm), which are not involved. This distortion of the ideal octahedral geometry of the $[SbF_6]^-$ anions goes along with deviations from the ideal 90 and 180° F-Sb-F angles up to 3.6(1) and 5.7(1)°, respectively.

Vibrational spectra of solid $[X_2SO_3F]^+[SbF_6]^-$ (X=H, D): The infrared and Raman spectra of $[H_2SO_3F]^+[SbF_6]^-$ and $[D_2SO_3F]^+[SbF_6]^-$ are shown in Figure 3, and the observed frequencies are summarized in Table 3 together with the quantum-chemical-calculated frequencies for

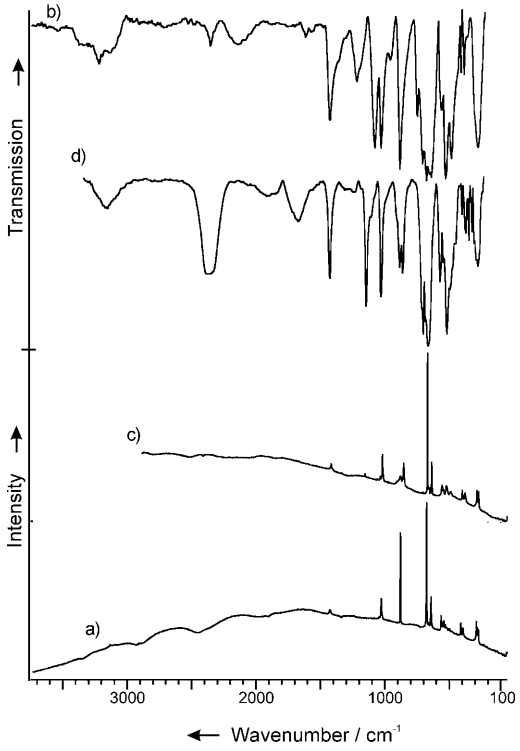

Figure 3. Vibrational spectra of $[H_2SO_3F]^+[SbF_6]^-$: a) Raman spectrum, b) IR spectrum; and of $[D_2SO_3F]^+[SbF_6]^-$: c) Raman spectrum, d) IR spectrum.

Table 3. Experimental vibrational frequencies [cm^{-1}] of $[X_2SO_3F]^+[SbF_6]^-$ and calculated vibrational frequencies [cm^{-1}] of $[X_2SO_3F(XF)_2]^+$ (X = H, D).

$[H_2SO_3F]^+[SbF_6]^-$ IR −80 °C	Raman −78 °C	$[H_2SO_3F(HF)_2]^+$ calcd[a]	$[D_2SO_3F]^+[SbF_6]^-$ IR −80 °C	Raman −78 °C	$[D_2SO_3F(DF)_2]^+$ calcd[a]	Assignment
–	–	3371 (126/120.5)	–	2447 (13, br)	2465 (66/5797)	ν_s(OX)
–	–	3332 (27503/7.4)	2355 (s)	2395 (10, br)	2426 (1486/4.0)	ν_{as}(OX)
1428 (s)	1425 (6)	1444 (353/4.9)	1427 (s)	1423 (17)	1443 (324/5.0)	ν(S=O)
1219 (m)	–	1211 (30/1.4)	–	–	–	δ_s(SOH)
–	–	1167 (225/0.5)	–	–	–	δ_{as}(SOH)
1080 (s)	1079 (3)	1013 (383/0.2)	1150 (s)	1156 (4)	1102 (278/1.1)	$\nu_{as}(SO_2)$
1029 (s)	1027 (15)	1015 (281/5.4)	1028 (s)	1022 (30)	1011 (287/5.6)	$\nu_s(SO_2)$
886 (vs)	879 (33)	899 (115/14.2)	883 (m)	882 (42)	901 (111/12.8)	ν(SF), ν_{breath}
–	–	–	859 (m)	856 (31)	864 (93/2.7)	δ_s(SOD)
–	–	–	–	–	840 (71/0.2)	δ_{as}(SOD)
551 (m)	549 (1)	593 (323/0.3)	–	–	–	$\delta(S(OH)_2)_{out\ of\ phase}$
–	541 (6)	539 (3/1.1)	–	–	–	$\delta(S(OH)_2)_{in\ phase}$
–	–	536 (32/1.9)	545 (sh)	545 (5)	532 (88/2.1)	δ(O=SF), $\delta(SO_2)$
525 (s)	530 (6)	518 (115/3.0)	496 (sh)	489 (8)	497 (116/3.3)	$\delta(SO_3)$
485 (s)	499 (5)	516 (0/1.9)	515 (vs)	524 (20)	514 (21/1.6)	$\delta(SO_3)$
–	–	–	400 (vw)	399 (10)	422 (84/0.6)	$\delta\ (S(OD)_2)_{out\ of\ phase}$
–	–	–			422 (5/0.2)	$d(S(OD)_2)_{in\ phase}$
411 (m)	410 (9)	403 (61/1.5)	371 (w)	378 (13)	380 (65/1.0)	$\delta(SO_2/OSF)_{scissor}$
386 (s)	393 (8)	361 (0/1.6)	345 (w)	–	326 (2/1.3)	$\delta(SO_2/OSF)_{waggingof\ phase}$
678 (vs)	675 (100)	–	667 (vs)	670 (100)	–	
640 (vs)	641 (16)	–	–	638 (29)	–	$[SbF_6]^-$
561 (m)	562 (9)	–	570 (m)	556 (18)	–	
273 (s)	275 (8)	–	280 (s)	274 (30)	–	

[a] Calculated at the RHF/6-311++G(d,p) level of theory. Frequencies were scaled with an empirical factor 0.92. IR intensity in km mol^{-1}. Raman activities in $Å^4 \mu^{-1}$.

$[X_2SO_3F(XF)_2]^+$. As shown by the crystal structure, the cation has C_1 symmetry. Therefore, it should exhibit 15 fundamental vibrations, which should be active in Raman as well as in infrared spectra. For the assignment of the vibrations the similar salt $[H_3SO_4]^+[SbF_6]^-$ and calculated frequencies for $[X_2SO_3F(XF)_2]^+$ have been considered. At this point it should be noted that the calculated $[X_2SO_3F(XF)_2]^+$ unit, which will be discussed later, represents the situation of the solid state better than a free $[X_2SO_3F]^+$ cation, since it takes into account the hydrogen bonds found in the crystal structure. The fifteen internal $[X_2SO_3F]^+$ vibrations have been depicted from the $[X_2SO_3F(XF)_2]^+$ unit by inspection of the Cartesian displacement coordinates of the vibrational modes.

Both infrared spectra of $[H_2SO_3F]^+[SbF_6]^-$ and $[D_2SO_3F]^+[SbF_6]^-$ show a broad band in the region above 3000 cm^{-1}, which is caused by traces of remaining moisture that is condensed onto the plates in the spectrometer during the measurements. Therefore, the deuterated species is more meaningful for the discussion of the O–X stretching modes of the cation. The O–D stretching modes are detected at 2447 (ν_{as}(OD)) and 2395 cm^{-1} (ν_s(OD)) in the Raman spectrum as broad lines, but only as one intense broad band at 2355 cm^{-1} in the infrared spectrum. Broad and intense O–X bands are expected as a result of the strong hydrogen bonds found in the crystal structure.[29] On the basis of the good agreement between experimental and calculated O–D stretching modes, the O–H stretching modes are expected to be close to the calculated frequencies at 3371 (ν_{as}(OH)) and 3332 cm^{-1} as broad bands that are additionally overlaid by the broad band of condensed moisture. However, an analysis of the water/ice band shape in the infrared spectrum indicates two additional bands that might be assumed to be O–H stretching modes of the $[H_2SO_3F]^+$ cation. Such an assignment is too uncertain and therefore has not been considered. Significant vibrational evidence for the O–H, as well as the O–D bonds, is given by the S-O-X deformation modes observed in the infrared spectra at 1219 and 859 cm^{-1}, respectively.

The S=O stretching mode is observed at nearly constant wavenumbers between 1423 and 1428 cm^{-1} for $[H_2SO_3F]^+$ and $[D_2SO_3F]^+$, respectively, and comparable to that observed for the $[H_3SO_4]^+$ cation (1401 cm^{-1}). This is expected due to the similarity of the cations and the absence of interionic interactions on this oxygen atom. A different situation is given for the S–O stretching vibrations. These are better described as modes between a sulfur atom and the hydroxy group, which itself participates in the O···X···F bridges found in the crystal structure. Overall, the symmetric and antisymmetric S–O stretching modes are observed in their typical regions and are comparable to the corresponding vibrations of the $[X_3SO_4]^+$ cations. Both vibrational modes are detected at a higher wavenumber than the S–O stretching vibration of fluorosulfuric acid (896 cm^{-1}).[14] This shift is usual, if one compares molecules and ions, since an increase of positive charge generally causes a blueshift of the vibrations. The trend is additionally overlaid by influences due to the O···X···F bridges and the isotopic H/D substitution. Thus, especially in the case of $\nu_{as}(SO_2)$, a remarkable shift between the deuterated and protonated cation is observed. This is in

accordance with the theoretical calculations and was similarly observed in the case of $[X_3SO_4]^+$.

The S–F stretching mode of the $[X_2SO_3F]^+$ cations is detected in a narrow region between 879 and 886 cm^{-1}. Compared with the neutral starting material HSO_3F with an S–F stretching mode at 830 cm^{-1}, the expected blueshift is observed. The moderate blueshift of 40 cm^{-1} as well as the narrow region of the S–F stretching modes of the cation support the crystallographic findings that the S–F bonds are not involved in interionic interactions. The deformation modes of the SO_3F skeleton are detected in the low wavenumber region below 545 cm^{-1}.

For an $[SbF_6]^-$ anion with ideal octahedral symmetry, two vibrations in the infrared and three vibrations in the Raman spectra with mutual exclusion are expected. For both the protonated and the deuterated salt, more vibrations are observed in the infrared and Raman spectra. This is in accordance with the lowered symmetry of the anion found in the crystal structure.

Theoretical calculations: Structure optimizations of the free $[H_2SO_3F]^+$ cation were performed by three different methods (fc-MP2, mPW1PW, and PBE1PBE) using the 6-311G-(3df,3pd) basis set.[30,31] Subsequently, vibrational frequencies in the harmonic approximation as well as IR and Raman intensities were calculated. The calculated bond lengths and angles of the free cation show a fair agreement with those experimentally found in the crystal structure (Table 4). The deviations are in the order of up to 2.5 pm for the S–O and S–F bonds, which is in the usual range,[32,33] but large differences occur between calculated and experimentally found vibrational frequencies. The O–X stretching vibrations especially were overestimated by up to 350 cm^{-1} compared with the experimental data. We assumed that these discrepancies were a result of the strong hydrogen bonds found in the crystal structure, since the formation of hydrogen bonds leads usually to a decrease of the corresponding O–X stretching frequency. To study the influence of hydrogen bonds in the calculations, we added two HF molecules to the free $[X_2SO_3F]^+$ cation. These $[X_2SO_3F(XF)_2]^+$ units were calculated by different methods (RHF 6-311++G(d,p), fc-MP2, and mPW1PW) using the 6-311++G(3df,3pd) basis set. The optimized structure of the $[X_2SO_3F(XF)_2]^+$ unit is shown in Figure 1. The calculated geometry of the $[X_2SO_3F(XF)_2]^+$ cation is comparable to that found in the crystal structure. The formal addition of HF molecules to the free cation leads to only small changes of the geometric parameters of the cation, but significantly influences the vibrational modes. In particular, the O–X stretching modes of the free cation are redshifted due to the formation of S–O···H···F–H hydrogen bonds into a region that already agrees fairly well with the experimental data. Overall, we find a satisfying agreement between the experimentally observed and calculated vibrational frequencies for the $[X_2SO_3F(XF)_2]^+$ cation, although the $[X_2SO_3F(XF)_2]^+$ unit represents a very simplified simulation of the solid state.

Table 4. Experimental geometric parameters for $[H_2SO_3F]^+[SbF_6]^-$ and calculated geometric parameters for $[H_2SO_3F(HF)_2]^+$ and $[H_2SO_3F]^+$.[a]

	$[H_2SO_3F]^+[SbF_6]^-$	$[H_2SO_3F(HF)_2]^+$		$[H_2SO_3F]^+$	
	exptl	RHF 6-311++G(d,p)	mPW1PW	PBE1PBE 6-311G(3df, 3pd)	fc-MP2
r(S=O)	139.5(2)	137.8	139.0	139.1	139.6
r(S–O)	147.5(3)/148.5(3)	148.9	150.8	150.8	151.0
r(S–F)	150.9(2)	150.4	150.7	150.7	151.0
r(O–H)	75.6(3)/93.1(2)	97.3	97.5	97.6	97.7
∢(O=S–F)	110.0(2)	110.4	111.7	111.6	111.6
∢(O=S–O)	119.1(2)/117.6(2)	118.5	118.9	119.0	119.3
∢(O-S-O)	103.3(1)	100.8	99.3	99.2	98.4
∢(O-S-F)	101.8(2)/102.7(1)	103.2	102.8	102.8	102.8
∢(S-O-H)	109.6(2)/120.6(2)	117.6	115.0	114.8	114.2

[a] Distances (*r*) are in pm and angles (∢) are in °.

Conclusion

The $[H_2SO_3F]^+$ cation was prepared and identified for the first time. The synthesis succeeded by the reaction of SO_3 with the superacidic solution HF/SbF_5 in which HSO_3F is formed in situ and instantly protonated. The resulting $[H_2SO_3F]^+[SbF_6]^-$ salt was characterized by its vibrational spectra and a single-crystal structure. In the solid state, strong hydrogen bonds (O···H···F) were observed between the cation and fluorine atoms of the anions. Therefore theoretical calculations of the free $[H_2SO_3F]^+$ cation did not describe the experimental vibrational spectra sufficiently. To consider influences by the hydrogen bridges, $[H_2SO_3F(HF)_2]^+$ was calculated, which contained two O···H···F contacts between the cation and the HF molecules. This simplified model of the solid state led to a sufficient agreement between calculated and experimentally found vibrational spectra as well as geometric parameters.

The successful synthesis of $[H_2SO_3F]^+[SbF_6]^-$ is in agreement with earlier studies, which indicated that the conjugated Brønsted–Lewis superacid HF/SbF_5 is more acidic than HSO_3F/SbF_5, since the more acidic superacid HF/SbF_5 protonated the weaker HSO_3F/SbF_5 system.

Experimental Section

Caution! Avoid contact with these compounds and note that the hydrolysis of $[SbF_6]^-$ salts forms HF, which burns the skin and causes irreparable

damage. Safety precautions should be taken when using and handling these materials.

Chemicals: SbF_5 (Merck) was distilled three times through Vigreux columns under a flow of dry nitrogen at atmospheric pressure and finally purified by trap-to-trap distillation under vacuum. HF (Messer Griesheim) was first trap-to-trap distilled under vacuum and then dried with fluorine for two weeks in a stainless steel pressure cylinder. DF was prepared from dried CaF_2 and D_2SO_4, distilled under vacuum, and dried with fluorine for two weeks in a stainless steel pressure cylinder. D_2SO_4 was obtained by a reaction of D_2O with SO_3, which was trap-to-trap condensed from oleum (65 % SO_3) (Merck).

Equipment and instrumentation: All synthetic work and sample handling were performed by employing standard Schlenk techniques and a stainless steel vacuum line. Superacid reactions were carried out in Kel-F ampoules, which were closed with stainless steel valves. All reaction vessels and the stainless steel line were dried with fluorine prior to use. Infrared spectra were recorded using a Bruker IFS 113v spectrophotometer in a cooled cell. Spectra of dry powders were obtained using a single-crystal silicon plate coated with the neat sample. The Raman spectra were recorded using a Jobin Yvon T64000 spectrometer with an Ar^+ laser tube (514.5 nm) from Spectra Physics. The spectra of the solids were recorded in a glass cell cooled with liquid nitrogen. Single crystals were placed in glass capillaries in a cooled stream of dry nitrogen, and the X-ray diffraction studies were carried out using an Enraf Nonius Kappa diffractometer with an Oxford Cryosystem cooling unit.

Synthesis of $[X_2SO_3F]^+[SbF_6]^-$ (X=D, H): In a typical reaction, XF (X = H, D; 3 g) was distilled into a Kel-F reactor at −196 °C, followed by SbF_5 (1 mmol, 220 mg). The mixture was warmed to 20 °C to form the superacid. The reactor was then cooled to −196 °C, and SO_3 (1 mmol, 110 mg) was condensed to the frozen superacid. The reaction mixture was warmed up to −35 °C for two minutes and then cooled to −78 °C. The excess of XF was removed in a dynamic vacuum at −78 °C. Colorless crystals (350 mg, 1 mmol; yield: 100 %) were obtained, which were suitable for X-ray diffraction studies.

Computational methods: The theoretical calculations were performed using the Gaussian 98 and Gaussian 03 programs[34] at different levels of theory using restricted Hartree–Fock (RHF) methods and the hybrid density functionals PBE1PBE and mPW1PW[35–38]. The 6-311++G(d,p) basis set was used in all calculations.[39,40] Pure functions (spherical harmonics) were used throughout to describe the angular part of the atomic basis function. Quadrature in all DFT calculations was performed on a pruned grid of 99 radial shells and 590 angular points per shell on each atom. Structural optimizations were performed using the GDIIS algorithm with tight (or very tight) convergence criteria, which corresponded to maximum deviations in density matrix elements of 10^{-6}, in the energy of 10^{-6} hartree, in the forces of 0.000015 (0.000002) hartree $bohr^{-1}$, and in atomic Cartesian displacements of 0.00006 (0.000006) bohr.[41]

Acknowledgements

This work was supported by the Deutsche Forschungsgemeinschaft and the Fonds der Chemischen Industrie.

[1] G. A. Olah, G. K. S. Prakash, J. Sommer in *Superacids*, Wiley, New York, **1985**.
[2] T. A. O'Donnell in *Superacids and Acidic Melts as Inorganic Chemical Reaction Media*, Wiley, New York, **1992**.
[3] G. A. Olah, G. K. S. Prakash, K. K. Laali in *Onium Ions*, Wiley, New York, **1998**.
[4] G. A. Olah, *Angew. Chem.* **1995**, *107*, 1519–1532; *Angew. Chem. Int. Ed.* **1995**, *34*, 1393–1405.
[5] R. Minkwitz, T. Hertel, *Z. Naturforsch. B* **1997**, *52*, 1283–1286.
[6] R. Minkwitz, S. Schneider, M. Seifert, *Z. Anorg. Allg. Chem.* **1996**, *622*, 1404–1410.
[7] R. Minkwitz, S. Schneider, *Angew. Chem.* **1999**, *111*, 229–23.
[8] R. Minkwitz, R. Seelbinder, R. Schöbel, *Angew. Chem.* **2002**, *114*, 119–121; *Angew. Chem. Int. Ed.* **2002**, *41*, 111–114.
[9] R. J. Gillespie, T. E. Peel, E. A. Robinson, *J. Am. Chem. Soc.* **1971**, *93*, 5083–5087.
[10] R. J. Gillespie, T. E. Peel, *J. Am. Chem. Soc.* **1973**, *95*, 5173–5178.
[11] R. J. Gillespie, *Acc. Chem. Res.* **1968**, *1*, 202–209.
[12] R. J. Gillespie, J. Liang, *J. Am. Chem. Soc.* **1988**, *110*, 6053–6057.
[13] K Bartmann, D. Mootz, *Acta Crystallogr. Sect. C* **1990**, *46*, 319–320.
[14] S. M. Chackalackal, F. E. Stafford, *J. Am. Chem. Soc.* **1966**, *88*, 4815–4819.
[15] R. J. Gillespie, E. A. Robinson, *Can. J. Chem.* **1962**, *40*, 644–657.
[16] P. Bernard, Y. Parent, P. Vasta, *C. R. Acad. Sci. Ser C* **1969**, *267*, 767.
[17] A. Ruoff, J. B. Milne, G. Kaufman, M. J. E. Leroy, *Z. Anorg. Allg. Chem.* **1970**, *372*, 119.
[18] Z. Dingliang, S. J. Rettig, J. Trotter, F. Aubke, *Inorg. Chem.* **1996**, *35*, 6113–6130.
[19] R. C. Thompson, J. Barr, G. J. Gillespie, J. B. Milne, R. A. Rothenbury, *Inorg. Chem.* **1965**, *4*, 1641–1649.
[20] A. Commeyras, G. A. Olah, *J. Am. Chem. Soc.* **1969**, *91*, 2929–2942.
[21] Z. Dingliang, M. Heubes, G. Hägele, F. Aubke, *Can. J. Chem.* **1999**, *77*, 1869–1886.
[22] J. Kühn-Velten, M. Bodenbinder, R. Bröchler, G. Hägele, F. Aubke, *Can. J. Chem.* **2002**, *80*, 1265–1277.
[23] Further details of the crystal structure investigation can be obtained from the Fachinformationszentrum Karlsruhe, 76344 Eggenstein-Leopoldshafen, Germany (fax: (+49)7247-808-666; e-mail: crysdata@fiz-karlsruhe.de) on quoting the depository number CSD-420516.
[24] Z. Otwinowski, W. Minor, *Methods Enzymol.* **1997**, *276*, 307–326.
[25] SHELXL 93, G. M. Sheldrick, Universität Göttingen, Göttingen, **1993**.
[26] SHELXL 86, G. M. Sheldrick, Universität Göttingen, Göttingen, **1986**.
[27] SHELXTL Plus Vers. 3.4, An integrated System for Solving, Refining and Displaying Crystal Structures from Diffraction Data, G. M. Sheldrick, Universität Göttingen, Göttingen, **1993**.
[28] A. Kornath, R. Seelbinder, R. Minkwitz, *Angew. Chem.* **2005**, *117*, 995–997; *Angew. Chem. Int. Ed.* **2005**, *44*, 973–975.
[29] J. Weidlein, U. Müller, H. Dehnicke in *Schwingungsspektroskopie*, Thieme, Stuttgart, **1988**.
[30] M. J. Frisch, J. A. Pople, J. S. Binkley, *J. Chem. Phys.* **1984**, *80*, 3265–3269.
[31] H. T. Clark, J. Chandrasekhar, G. W. Spitznagel, P. von R. Schleyer, *J. Comput. Chem.* **1983**, *4*, 294–301.
[32] F. Jensen in *Introduction to Computational Chemistry*, Wiley, New York, **1999**.
[33] I. N. Levine in *Quantum Chemistry*, 5th ed., **1999**, Prentice Hall, New York.
[34] Gaussian 03, Revision D.01, M. J. Frisch, G. W. Trucks, H. B. Schlegel, G. E. Scuseria, M. A. Robb, J. R. Cheeseman, J. A. Montgomery, Jr., T. Vreven, K. N. Kudin, J. C. Burant, J. M. Millam, S. S. Iyengar, J. Tomasi, V. Barone, B. Mennucci, M. Cossi, G. Scalmani, N. Rega, G. A. Petersson, H. Nakatsuji, M. Hada, M. Ehara, K. Toyota, R. Fukuda, J. Hasegawa, M. Ishida, T. Nakajima, Y. Honda, O. Kitao, H. Nakai, M. Klene, X. Li, J. E. Knox, H. P. Hratchian, J. B. Cross, V. Bakken, C. Adamo, J. Jaramillo, R. Gomperts, R. E. Stratmann, O. Yazyev, A. J. Austin, R. Cammi, C. Pomelli, J. W. Ochterski, P. Y. Ayala, K. Morokuma, G. A. Voth, P. Salvador, J. J. Dannenberg, V. G. Zakrzewski, S. Dapprich, A. D. Daniels, M. C. Strain, O. Farkas, D. K. Malick, A. D. Rabuck, K. Raghavachari, J. B. Foresman, J. V. Ortiz, Q. Cui, A. G. Baboul, S. Clifford, J. Cioslowski, B. B. Stefanov, G. Liu, A. Liashenko, P. Piskorz, I. Komaromi, R. L. Martin, D. J. Fox, T. Keith, M. A. Al-Laham, C. Y. Peng, A. Nanayakkara, M. Challacombe, P. M. W. Gill, B. Johnson, W. Chen, M. W. Wong, C. Gonzalez, J. A. Pople, Gaussian, Inc., Wallingford CT, **2004**.
[35] W. J. Hehre, L. Radom, P. V. Schleyer, J. A. Pople in *Ab initio Molecular Orbital Theory*, Wiley-Interscience, New York, **1986**.
[36] C. Møller, M. S. Plesset, *Phys. Rev.* **1934**, *46*, 618–622.

[37] C. Adamo, V. Barone, *J. Chem. Phys.* **1998**, *108*, 664–675.
[38] a) M. Ernzerhof, G. E. Scuseria, *J. Chem. Phys.* **1999**, *110*, 5029–5036; b) C. Adamov, V. Barone, *Chem. Phys. Lett.* **1998**, *298*, 113–119.
[39] R. Krishnan, J. S. Binkley, R. Seeger, J. A. Pople, *J. Chem. Phys.* **1980**, *72*, 650–654.
[40] A. D. McLean, G. S. Chandler, *J. Chem. Phys.* **1980**, *72*, 5639–5648.
[41] P. Császár , P. Pulay, *J. Mol. Struct.* **1984**, *114*, 31–34.

Received: March 24, 2009
Revised: September 5, 2009
Published online: November 26, 2009

